



5th International Conference on Silicon Photovoltaics, SiliconPV 2015

Base contacts and selective emitters processed by laser doping technique for p-type IBC c-Si solar cells

Gema López*, Pablo R. Ortega, Isidro Martín, Cristóbal Voz, Anna B. Morales, Albert Orpella, Ramón Alcubilla

Departament d'Enginyeria Electrònica, Universitat Politècnica de Catalunya, C/Jordi Girona 1-3, Mòdul C4, 08034 Barcelona, Spain

Abstract

In this work, we describe a novel fabrication process of p-type interdigitated back contact (IBC) silicon solar developed by means of laser doping and laser firing techniques. We use dielectric layers both as dopant sources to create highly-doped regions and as passivating layers. In particular, we use phosphorus-doped silicon carbide stacks ($a\text{-SiC}_x$ (n)) deposited by Plasma Enhanced Chemical Vapor Deposition (PECVD) and aluminum oxide (Al_2O_3) layer deposited by atomic layer deposition (ALD). Emitters were fabricated with a light thermal phosphorus diffusion in order to reduce bulk and surface emitter recombination losses. Highly doped regions n^{++} (emitter) and p^{++} (base) were simultaneously created in a point-like structure using a pulsed Nd-YAG 1064 nm laser in the nanosecond regime by laser processing the dielectric layers. The results obtained for a cell, $3 \times 3 \text{ cm}^2$, are presented. Efficiencies up to 18.1% ($J_{sc} = 39 \text{ mA/cm}^2$, $V_{oc} = 632 \text{ mV}$, $FF = 73.4\%$) have been achieved in our fabricated IBC cells.

© 2015 The Authors. Published by Elsevier Ltd. This is an open access article under the CC BY-NC-ND license (<http://creativecommons.org/licenses/by-nc-nd/4.0/>).

Peer review by the scientific conference committee of SiliconPV 2015 under responsibility of PSE AG

Keywords: IBC-BJ; Laser doping, selective emitter, c-Si solar cells

* Corresponding author. Tel.: +34-93-4015671; fax: +34-93-4016756.
E-mail address: gema.lopez@upc.edu

1. Introduction

Interdigitated Back-Contact (IBC) back-junction solar cells exhibit both emitter and base contacts on the back side of the cell which provides some advantages over front side contacted solar cells, e.g., simpler interconnection techniques and higher packing density [1], zero shading losses, resistive losses in the metal grid are significantly reduced, light trapping and front surface passivation aesthetics can be optimized, among other [2]. However, IBC solar cells require high minority carrier lifetime in the silicon bulk (τ_{bulk}) to avoid the recombination of the minority carriers generated that diffuse through the wafer thickness and are collected at interdigitated junctions on the rear side of the cell. Another requirement is low front surface recombination velocity (S_{front}). A poorly passivated front surface causes high recombination rates of the carriers photogenerated close to the front side where the most part of the photogeneration takes place. Both requirements are needed in order to reach high efficiency devices [3],[4]. One of the challenges related with the fabrication process is to ensure high bulk lifetime during the entire manufacturing procedure (no contamination and free-damage process) and low surface recombination velocities using a cost-effective processing.

The manufacturing processes used to fabricate IBC cells tend to be complicated and expensive often related to high temperature processing steps and patterned methods such as photolithography. The use of laser processes to create doped regions into crystalline silicon (c-Si) can significantly reduce the global thermal budget during the fabrication of solar cells.

Laser doping processes can employ phosphosilicate glass grown on c-Si surface during the conventional diffusion [5], [6], spin-on dopant [7],[8] or chemical liquid as a doping source [9],[10]. Dielectric layers like phosphorus-doped silicon nitride, phosphorus-doped silicon carbide or aluminium oxide have been previously used for the creation doped region by means of laser [11], [12],[13]. In the last years our research group (Micro and Nanotechnologies, MNT) at the UPC has developed and optimized two laser processes on phosphorus-doped silicon carbide stack SiC_x (referred as SiC_x (n) from now on) for the creation of n^+ region [14] and successfully applied to the rear contact of heterojunction solar cell [15], [16] and aluminium oxide (Al_2O_3) for p^+ region with excellent results [17],[18]. The DopLa (Doped by Laser) cell concept was the result of combining both techniques [19].

In this work we report on IBC cells where both p^{++} base and n^{++} emitter contacts are performed in one single-laser step using dielectric layers deposited at low temperature as doping sources (i.e., Al_2O_3 and SiC_x (n) respectively). Additionally, these layers provide surface passivation and reduce back optical reflectance if the thickness is adequately tuned [20]. Combining these dielectric layers with laser process has the potential to drastically simplify the fabrication of IBC c-Si solar cells.

2. Device structure and fabrication

A cross-section sketch of the developed IBC cell is shown in Fig.1. These cells were fabricated on p-type float-zone (FZ) silicon wafers. The starting thickness was $275 \pm 10 \mu\text{m}$ and the base resistivity $2.5 \pm 0.5 \Omega\text{cm}$.

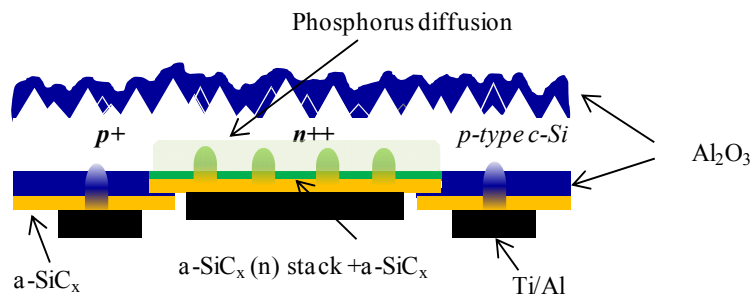


Fig. 1. Cross-section sketch of a p-type IBC processed solar cell.

The fabrication starts with a light thermal diffusion performed at 840 °C from solid source and a subsequent O₂ drive-in (1080 °C) resulting a n⁺ emitter with 135 Ω/sq sheet resistance. Next, a dry thermal oxidation is carried out in order to grow a SiO₂ layer to protect the rear side from the subsequent front side random texturation achieved by tetramethyl ammonium hydroxide (TMAH) solution. After remove the back SiO₂ masking layer, we deposit in the whole rear side by PECVD a dielectric a-SiC_x (n) stack. This stack consist of Si-rich intrinsic SiC_x passivating layer (~ 4 nm), a phosphorus-doped amorphous silicon layer (~ 15 nm) and a stoichiometric a-SiC_x 25 nm thick film (n = 2.0 at 632 nm) for chemical protection purposes. Emitter is defined through photolithography followed by CF₄ and isotropic etching. After an RCA cleaning, we deposit 90 nm of Al₂O₃ by thermal-ALD (atomic layer deposition) at 200°C on both sides. This layer plays the role of passivating front layer and antireflection coating Base regions are created by etching the Al₂O₃ from the emitter region through photolithography step. In this case the Al₂O₃ rear layer provides rear surface passivation and aluminum atoms for the p⁺⁺ region formation. An additional stoichiometric a-SiC_x film (50 nm thick) is deposited on the entire device rear side to optimize the back reflector. Next, the rear of the solar cells are irradiated applying a pulsed Nd-YAG 1064 nm laser in the nanosecond regime in a point-like structure. In this way, laser beam simultaneously ablates the dielectric layers and diffuses the dopant atoms creating highly doped n⁺⁺ and p⁺⁺ regions. These highly doped regions underneath the contacts helps for the formation of a good ohmic contact. The rear side is totally covered by e-beam evaporated Ti/Al film stack. A photolithography step and Ti and Al etching defined both emitter and base metal buses in an interdigitated pattern. Finally, an annealing at 400 °C for 10 min in H₂/N₂ atmosphere recovers the damage produced during the e-beam evaporation and activates the negative charge in the Al₂O₃/c-Si interface [21]. A schematic fabrication process is presented in Fig.2.

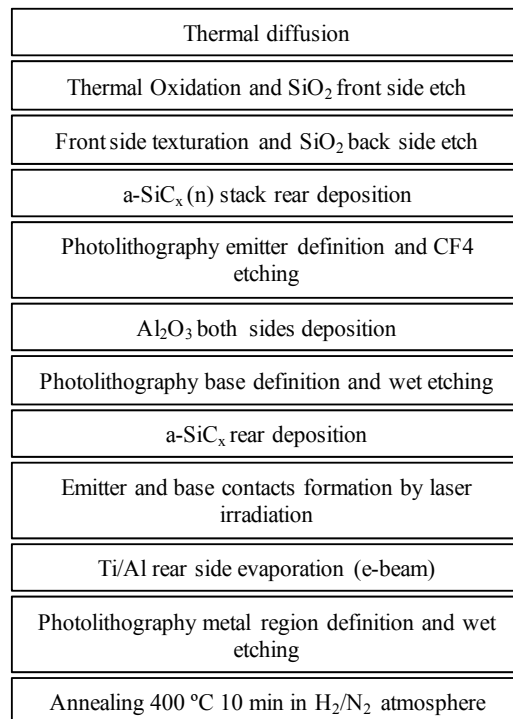


Fig 2. Fabrication process scheme IBC solar cell

Laser spots are defined in a square matrix shape with a pitch of 250 μm because the optimal trade-off between base resistance and carrier collecting losses as explained in [22]. Additionally a 75% emitter coverage has been considered in our devices. Laser doping was carried out using a pulsed Nd:YAG laser (StarMark SMP100 II Rofin-

Baasel) working at 1064 nm wavelength in TEM00 mode, with a frequency of 4 KHz and the pulse duration of 100 ns. Regarding the beam characteristics, an objective lens with a focal length of 31.4 cm is used leading to a beam waist of 70 μm radius with a Gaussian profile and a round shape (Fig.3). The energy of the laser beam was adjusted by varying the intensity of the continuous lamp that pumps the Nd:YAG crystal. In this study, the laser power is fixed at 0.9 W and 6 pulses per spot resulting in a 60 μm diameter laser spot on the dielectric films.

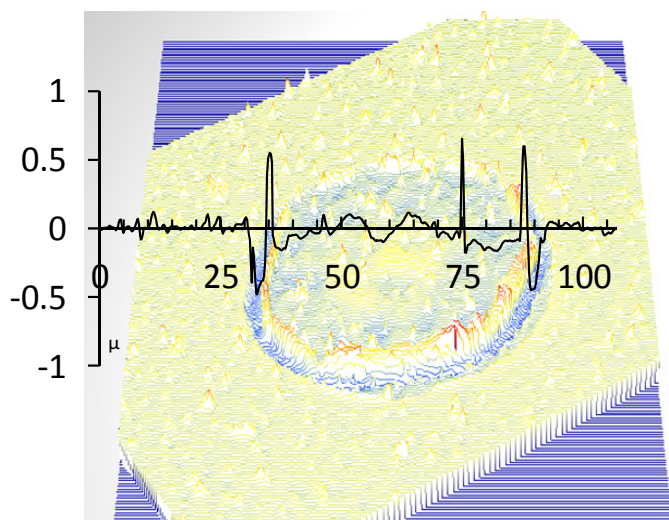


Fig 3. Laser spot interferometry done at 0.9 W. Inset curve of profilometric measurement.

3. Results and discussion

3.1. Texturing, front and antireflection coating

In order to study the reflectance and the passivation quality, a c-Si sample was symmetrically prepared with double-side random texturation and 90 nm of Al_2O_3 . Reflectance was measured by UV-VIS-NIR spectrophotometer and the effective minority carrier lifetime (τ_{eff}) by quasi-steady-state photoconductance (QSSPC) method using WTC-120 apparatus from Sinton Consulting. In Fig. 4 we report the reflectance spectra and the effective minority carrier lifetime measurements.

The textured sample exhibits an integrated average reflectance of 13% in front of the polished c-Si (37%). Further reduction of the reflectance below 1% (from 450 to 1000 nm) is achieved when the textured c-Si is coated by the passivating layer which also acts as antireflection coating (ARC).

An optical bandgap of $E_{\text{opt}} = 6.4 \pm 0.1$ eV for annealed ALD Al_2O_3 films has been previously reported [23]. Therefore, scarcely light absorption occurs by the film in the wavelength range relevant for photovoltaic applications. This layer also provides an excellent passivation behavior and after an annealing step at 400 $^{\circ}\text{C}$ for 10 min in a forming gas atmosphere the passivation quality is clearly enhanced. The τ_{eff} increases up to 1.2 ms at 1-sun injection level (indicated by an arrow in the figure). The upper limit of the surface recombination velocity ($S_{\text{eff,max}}$) can be calculated (assuming an infinite bulk lifetime due to the high quality p-type FZ-Si used) as follow:

$$S_{\text{eff,max}} = \frac{W}{2 \times \tau_{\text{eff,1sun}}}$$

where W (~ 275 μm) is the sample thickness. Values of $S_{\text{eff,max}} < 15$ cm/s at 1-sun illumination have been obtained.

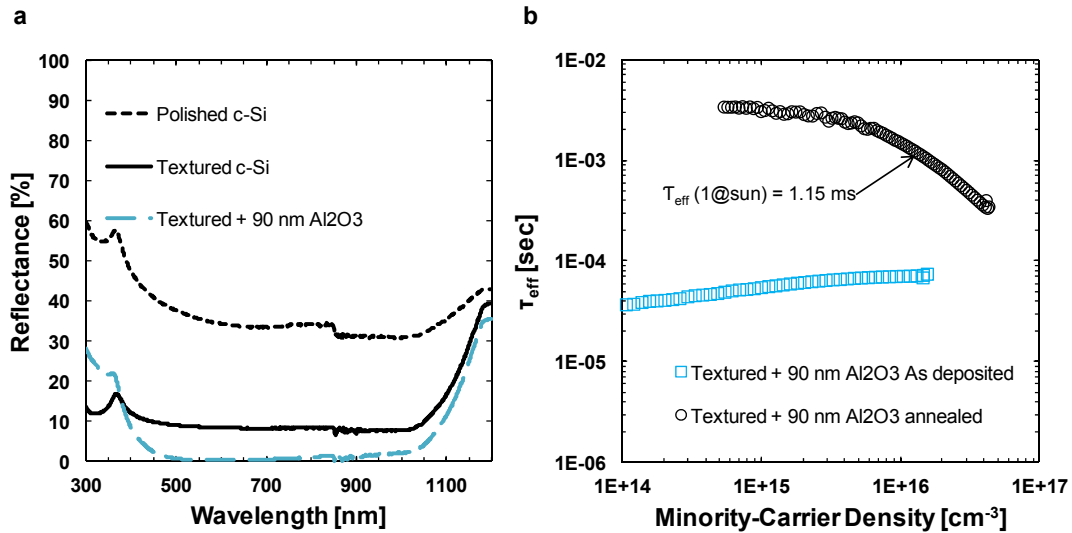


Fig 4.(a) Reflectance curves of 90 nm Al₂O₃-coated randomly textured c-Si (blue long dash), textured c-Si (black line) and bare polished c-Si as a reference (short dash); (b) τ_{eff} vs. excess carrier density for symmetrical sample double-side textured and covered by 90 nm of Al₂O₃ as-deposited and after annealing step.

3.2. Joe, EQE and V-J measurements

Emitter saturation current (J_{oe}) was determined measuring effective lifetime on a symmetrical c-Si sample processed in the same way as the IBC emitter. Test structure n+pn+ is shown in Fig. 5a. Lifetime is measured before laser processing. Then, we irradiate only one surface with laser spots with a pitch of 250 μm covering 4.5% of the total surface area and τ_{eff} was measured again. J_{oe} was extracted from the slope of the $1/\tau_{\text{eff}}$ vs. Δn (excess carrier density, cm⁻³) at high injection (Fig. 5b) using the method proposed by Kane and Swanson [23]. Emitter saturation currents of 36 fA/cm² and 42 fA/cm² were obtained before and after laser process respectively. Therefore a J_{oe} can be deduced for each selective emitter point yielding $\sim 150 \text{ fA/cm}^2$.

Despite the J_{oe} does not change much before and after laser process, there is a degradation of the bulk lifetime as it can be deduced from the shift at low injection level between the graphs (Fig. 5b). This deterioration has probably been caused by the damage into the bulk lattice during the laser doping stage.

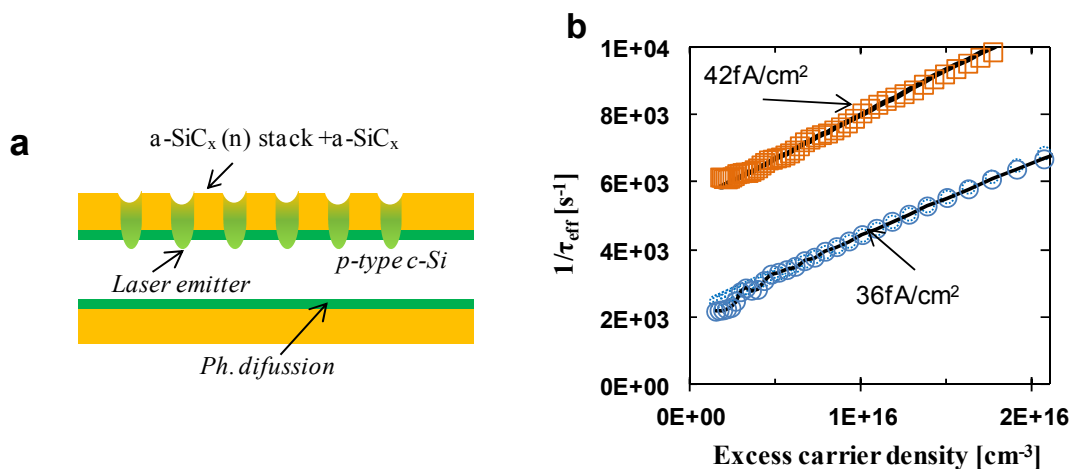


Fig 5. (a) Symmetrical test structure for measurements of minority carrier lifetime. (b) Determination of J_{oe} using the 'slope method' for a symmetrical sample before (blue round- shape) and after laser process (orange square-shaped) where a point-like selective emitter is created

In Fig. 6a, current and power as a function of applied voltage for our IBC is shown. Photovoltaic parameters were measured under standard conditions (AM1.5g, 100 mW/cm², 25 °C) and are summarized in the inset. Photovoltaic efficiency η , open-circuit voltage V_{oc} , short-circuit current density J_{sc} and fill factor FF of 18.1%, 632 mV, 39 mA/cm² and 73.4% respectively have been obtained. Additionally, external quantum efficiency EQE higher than 95% in the 500-1000 nm wavelength range (see Fig. 6b). The high J_{sc} value confirms that excellent surface passivation is achieved in our devices.

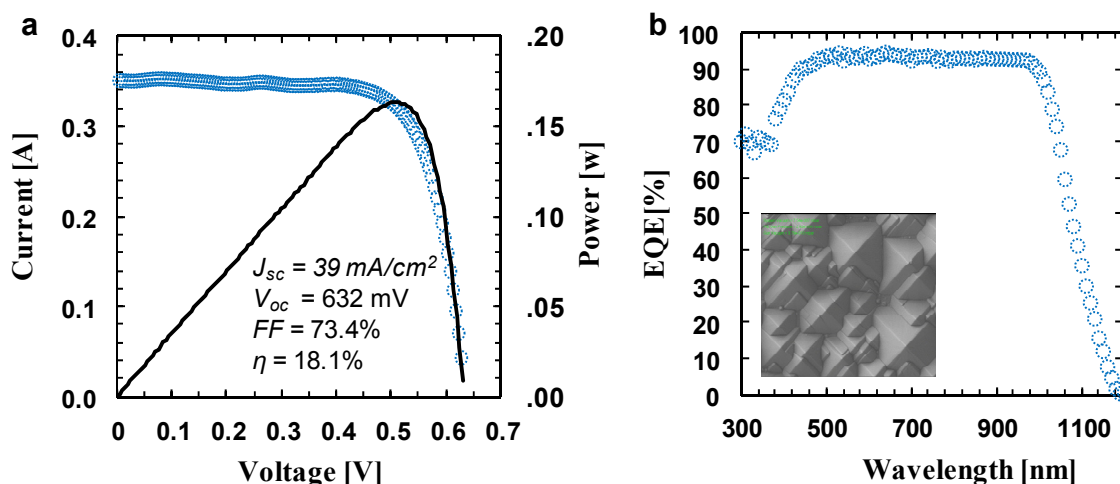


Fig 6.(a) I-V and P-V curves of the IBC cell with an area of 9 cm² and emitter coverage of 75%. Measurements under AM1.5G at 25 °C. Inset electrical parameters measured. (b) EQE vs. wavelength at 0.3 suns. A SEM image of random pyramids is shown in the inset.

However, the relatively low V_{oc} seems to be due to a high effective surface recombination velocity at the laser doped p+ contacts once metalized ($\sim 5 \times 10^4$ cm/s) as it is suggested in our previous work [24].

4. Conclusions

In this work we present the fabrication process of p-type IBC solar cell based on laser processing of Al₂O₃/a-SiC_x and a-sSiC_x(n) stack films. We have demonstrated a front $S_{eff,max}$ less than 15 cm/s that fulfills the requirement to achieve high efficiency IBC. Furthermore, the front surface texturation in combination with the Al₂O₃, which acts also as antireflection film, provides a reflectance below 1% in the wavelength range relevant for photovoltaic applications.

On the other hand, it has also been demonstrated that these dielectric films can be used as dopant sources of aluminium for BSF and phosphorus for the selective emitter creation. Efficiency higher than 18% has been achieved as a proof of concept. This study paves the way for future studies focused on IBC fabrication using only dielectric layers. The global thermal budget could be reduced by avoiding the high temperature diffusion process.

Acknowledgements

This work has been supported by the Spanish Government under project TEC 2011-26329, ENE2013-48629-C4-1-R and by the European Union's Seventh Framework Programme for research, technological development and demonstration under project HERCULES (Grant agreement:608498).

References

- [1] Kress A, Breitenstein O, Glunz S, Fath P, Willeke G, Bucher E. Investigations on low-cost back-contact silicon solar cells. *Sol Energy Mater Sol Cells*. 2001;65(1):555–60.
- [2] Zin N, Blakers A, McIntosh KR, Franklin E, Kho T, Chern K, et al. Continued Development of All-Back-Contact Silicon Wafer Solar Cells at ANU. *Energy Procedia* 2013;33:50–63.
- [3] Van Kerschaver E, Beaucarne G. Back-contact solar cells: A review. *Progress in Photovoltaics: Research and Applications*. 2006. p. 107–23.
- [4] Chan C.E, Hallam B.J, Wenham S.R. Simplified Interdigitated Back Contact Solar Cells. *Energy Procedia* 2015;27:543–8.
- [5] Okanovic M, Jäger U, Ahrens M, Stute U. Influence of different laser parameters in laser doping from phosphosilicate glass; In: *Proceeding of 24th European Photovoltaic Solar Energy Conference*, Hamburg, Germany, 2009; 24-27
- [6] Werner J.H, Röder T.C, Eisele S.J, Grabitz P, Köhler J.R. Laser Doped Selective Emitters Yield 0.5% Efficiency Gain. In: *Proceeding of 24th European Photovoltaic Solar Energy Conference*, Hamburg, Germany, 2009;1847-1850
- [7] Colina.M., Martín I., Voz C., Morales-Vilches A., Ortega P., López G., Orpella A., Alcubilla R, Sánchez-Aniorte I. Molpeceres C., Optimization of laser doping processes for the creation of p+ regions from solid dopand sources; In: *Proceeding of 27th European Photovoltaic Solar Energy Conference*, Frankfurt, Germany, 2012; 1885-1889.
- [8] Ogane A, Hirata K, Horiuchi K, Kitiyanan A, Uraoka Y, Fuyuki T. Feasible control of laser doping profiles in silicon solar cell processing using multiple excitation wavelengths. *33rd IEEE Photovolt Spec Conf.*, 2008;
- [9] Kray D., Fell A., Hopman S., Mayer K., Willeke G. and Glunz S.W. Laser chemical processing (LCP). A versatile tool for microstructuring applications. *Appl Phys A Mater Sci Process.*, 2008;93:99–103.
- [10] Kray D, McIntosh K.R. Analysis of Selective Phosphorous Laser Doping in High-Efficiency Solar Cells. *IEEE Trans Electron Devices* 2009;56(8):1645–50.
- [11] Paviet-Salomon B, Gall S, Monna R, Manuel S, Slaoui A, Vandroux L, et al. Laser doping using phosphorus-doped silicon nitrides. *Energy Procedia* 2011;8:700–5
- [12] Suwito D, Jager U, Benick J, Janz S, Hermle M, Glunz S.W. Industrially Feasible Rear Passivation and Contacting Scheme for High-Efficiency n-Type Solar Cells Yielding a V_{oc} of 700 mV; *IEEE Trans Electron Devices* 2010;57(8):2032–6.
- [13] Fell A., Franklin E., Walter D., Suh D., Weber K.J. Laser doping from Al_2O_3 layers. In: *Proceeding of 27th European Photovoltaic Solar Energy Conference and Exhibition*; Frankfurt, Germany 2012; 706–708.
- [14] López G, Ortega P, Colina M, Voz C, Martín I, Morales-Vilches A, et al. Emitter formation using laser doping technique on n- and p-type c-Si substrates. *Appl Surf Sci* 2014, <http://dx.doi.org/10.1016/j.apsusc.2014.10.140>
- [15] Morales-Vilches A, Voz C, Colina M, Lopez G, Martín I, Orpella A, et al. Progress in silicon heterojunction solar cell fabrication with rear laser-fired contacts. *Proceedings of the 2013 Spanish Conference on Electron Devices, CDE 2013*, 2013; 345–8.
- [16] Martín I., Colina M., Orpella A, Voz C., De Vecchi S., Desrués T., Abolmasov S., Roca i Cabarrocas P, et al. Low Recombination n+ Regions Created by n+ c-Si Epitaxial Layers and Laser Processing of Phosphorus-Doped SiCx Films. In: *Proceeding of 27th European Photovoltaic Solar Energy Conference and Exhibition*; Frankfurt, Germany 2012;1519–23.
- [17] Martín I, Ortega P, Colina M, Orpella A, López G, Alcubilla R. Laser processing of $Al_2O_3/a-SiC_x:H$ stacks: a feasible solution for the rear surface of high-efficiency p-type c-Si solar cells. *Prog Photovoltaics Res Appl*, 2013; 21; 1171-1175
- [18] Ortega P, Martín I, Lopez G, Colina M, Orpella A, Voz C, et al. p-type c-Si solar cells based on rear side laser processing of $Al_2O_3/SiCx$ stacks. *Solar Energy Materials and Solar Cells* 2012; 80–3.
- [19] Martín I., Colina M., Coll A., López G., Ortega P. Orpella A., Alcubilla R.; c-Si solar cells based on laser-processed dielectric films. In: *Proceeding of 4th International Conference on Silicon Photovoltaics, Silicon PV*. *Energy Procedia* 2014.
- [20] López G., Ortega P., Voz C., Martín I., Colina M., Morales-Vilches A., Orpella A., Alcubilla R.; Surface passivation and optical characterization of $Al_2O_3/a-SiC_x$ stacks on c-Si substrates. *Beilstein J Nanotechnol*. 2013;4:726–31.
- [21] Werner F, Veith B, Tiba V, Poodt P, Roozeboom F, Brendel R, et al. Very low surface recombination velocities on p- and n-type c-Si by ultrafast spatial atomic layer deposition of aluminum oxide. *Appl Phys Lett* 2010; 97(16):162103.
- [22] Carrio D., Ortega P., Martín I., López G., López-González J.M., Orpella A., Voz C., Alcubilla R.; Rear contact pattern optimization on 3D simulations for IBC solar cells with point-like doped contacts; In: *proceeding of 4th Int Conf Silicon Photovoltaics, Silicon PV*; *Energy Procedia* 2014;.
- [23] Kane D.E, Swanson R.M. Measurement of the Emitter Saturation Current by a Contactless Photoconductivity Decay Method. *Proceedings of the 18th Photovoltaic Specialists Conference. IEEE Operations Center* 1985; 578–83.
- [24] López-González J., Martín I, Ortega P., Orpella A., Alcubilla R.; Numerical simulations of rear point-contacted solar cells on 2.2 Ω cm p-type c-Si substrates; *Pro. Photovolt: Res.Appl*. 2013; 23; 69-77.